ChemPubSoc Europe

DOI: 10.1002/chem.201403998

CHEMISTRY A European Journal Full Paper

Self-Assembly

The Readout of Base-Pair Information in Adenine–Thymine α-D-Arabinonucleosides

Shiliang He,[a] Hang Zhao,[a, b] Xiurong Guo,[a] Xiaoping Xu,[b] Xinglong Zhou,[a] Jiang Liu,[a, b] Zhihua Xing,[a] Ling Ye,[b] Lu Jiang,[b] Qianming Chen,*[b] and Yang He*[a]

Abstract: Structurally modified nucleosides are central players in the field of nucleic acid chemistry. Adenine–thymine (AT) pyrimido[4,5-d]pyrimidine furanosyl and pyranosyl arabinonucleosides have been synthesized for the first time. Single-crystal X-ray diffraction analysis reveals novel base pairs that, in synergy with the sugar residues, direct the emergence of distinct networks containing channels and cavities. The microscopic noncovalent connections can be translated into macroscopic levels in which robust organogels are formed by the furanoside but not the pyranoside. The influences of the sugars are also displayed by the different shaped superstructures of the free nucleosides in solution. The readout of the information in the base moiety is therefore tailored by the sugar configuration, and the interplays exert subtle effects on the structures, from solid to gel and to the solution state. The potential for forming these appealing base pairs and higher structures enables these intriguing nucleosides to serve as unique building blocks in various areas or to construct innovative nucleic acid structures.

Introduction

The elucidation of the double-helix structure of DNA[1] by Watson and Crick, based on Chargaff's observation of the equal ratios of purines and pyrimidines in DNA and the X-ray data of Franklin and Wilkins, has brought about explosive advances in various scientific fields. In particular, the establishment of the base-pair-based flow of genetic information in processes of replication, transcription, and translation has revolutionized many aspects of biology. Apart from biological areas, chemists' attempts to exploit the diverse structures and the rich chemistry from both the sugar residues and the heterocyclic moieties of nucleosides/nucleotides/nucleic acids to create unnatural entities with various properties have accelerated the evolution from genetic to generic materials that cross many areas of chemistry, including basic research[2] and medicinal[3] and nanotechnology applications.[4] The systematic investigation of Eschenmoser and co-workers on the chemical etiology of the nucleic acid structure (by using four- to six-carbon saccharides as backbones) offered insights into Nature's choice of pentose over other sugar alternatives as the carbohydrate building block for the genetic system.[2b–f] The focus on the diversities of base-pair motifs[2g] expanded the genetic alphabet by enzymatically incorporating different artificial base-modified nucleosides into genomes.[2h,i] Certain types of nucleoside analogues have been developed into efficient therapeutic agents against tumors and viruses by modifing the sugar and/or base moieties.[3] The specific molecular recognition of nucleobases has been explored extensively to construct nanoscale architectures ranging from monomeric supramolecular complexes[4a–f] to polymeric DNA origami.[4g,h] Inspired by these works and especially fired up by Lehn and co-workers' research on the rosette structure of the Janus type guanine–cytosine (J-GC) base,[4a] we have synthesized tridentate (J-GC) and bidentate (J-adenine–thymine, J-AT) ribonucleosides and evaluated their biological and supramolecular self-assembly properties.[5] Differences in the hydrogen-bonding patterns of the base pair and/or the position of glycosylation led to different supramolecular nanoflowers or nanobundles in the solution state.[5c,d] Later on, we found that both the sugar and base components and the interplay between them were deterministic factors for the complex self-assembly of J-AT derivatives.[5f] This drove us to expand our study to other sugar systems as a part of systematic investigation. With the consideration that arabinose is the epimer of ribose with the reversed configuration at the first chiral center and given the biological/medicinal importance of arabinonucleosides,[6] it was logical for us to select this sugar as the first candidate.

During the initial design, the bidentate adenine–thymine nucleosides were thought to form either Watson–Crick or reverse Watson–Crick base pairs, which would lead to either a cyclic

[a] S. He,[+] Dr. H. Zhao,[+] Dr. X. Guo,[+] X. Zhou, J. Liu, Z. Xing, Prof. Dr. Y. He
Institute for Nanobiomedical Technology and Membrane Biology
Regenerative Medicine Research Center, West China Hospital
West China Medical School, Sichuan University
No. 1, Keyuan 4th Road, Gaopengdadao, Chengdu 610041 (China)
E-mail: heyangqx@scu.edu.cn

[b] Dr. H. Zhao,[+] X. Xu, J. Liu, Prof. Dr. L. Ye, Prof. Dr. L. Jiang, Prof. Dr. Q. Chen
State Key Laboratory of Oral Diseases
West China Hospital of Stomatology, Sichuan University
No. 14, Section 3, Renminnan Road, Chengdu 610041 (China)
E-mail: qmchen@scu.edu.cn

[+] These authors contributed equally to this work.

Supporting information for this article is available on the WWW under http://dx.doi.org/10.1002/chem.201403998.

© 2014 Wiley-VCH Verlag GmbH & Co. KGaA, Weinheim

structure or a linear structure (Figure S1 in the Supporting Information). Afterwards, the experimental evidence revealed that reverse Watson–Crick base pairs are indeed formed by sugar-protected or free J-AT ribonucleosides. Thus, we supposed that the corresponding arabinonucleosides would also form the same base pairs because the base moiety stores the same information of hydrogen-bonding patterns. Surprisingly, completely different scenarios were observed: the neighboring amino group of the adenine ring and oxo group of the thymine ring form a quasi-Hoogsteen face to participate in the base-pair formation, and the N1 atom of the thymine ring is also a potential acceptor site. Herein, we report the critical details of how the readout of the information stored in the base moiety (by which face to form base pairs) is tailored by the spatial arrangements of the sugar substituents and how the microscopic interactions can be translated into higher structures.

Results and Discussion

Synthesis and monomeric structures

To synthesize the J-AT arabinonucleoside, we adopted the Vorbrueggen (or silyl-Hilbert–Johnson) reaction[7] by coupling silylated J-AT base moiety **4** with the corresponding arabino-sugar donor in the presence of Friedel–Crafts catalyst (Scheme 1).

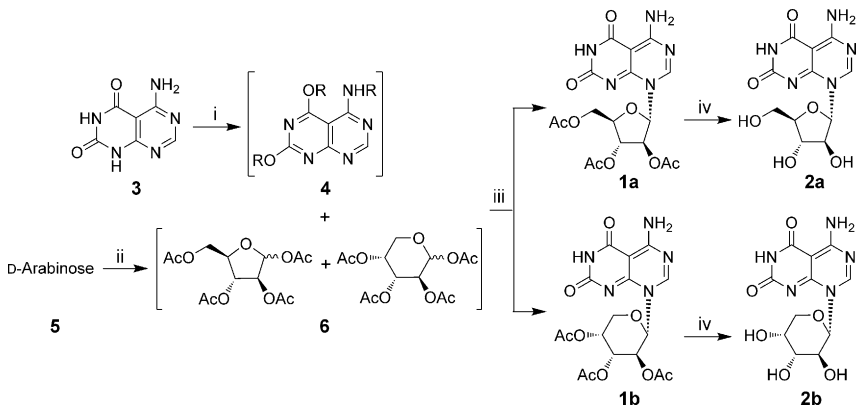

Scheme 1. Synthesis of J-AT α-D-arabinonucleoside analogues **1a**, **1b**, **2a**, and **2b**. R: TMS. i) HMDS, TMSCl, reflux; ii) Ac_2O, NaOAc, 110 °C, 96%; iii) dry acetonitrile/dry 1,2-dichloroethane (1:1), $SnCl_4$, 80 °C, 3 h, 52% total yield; iv) 0.2 M MeONa/MeOH, reflux, 72% for **2a**, 70% for **2b**. TMS: trimethylsilyl; HMDS: hexamethyldisilazane.

The sugar donor, per-O-acetylated D-arabinose, was obtained in a one-pot reaction by direct acetylation of D-arabinose in hot acetic anhydride in the presence of sodium acetate.[8] This straightforward route is much shorter than the generally adopted three-step Guthrie–Smith method[9] but has not yet been commonly employed in the synthesis of peracetylated arabinose. Next, this syrup was coupled with silylated base moiety **4** with $SnCl_4$ as the catalyst because it gave a much higher yield than the weaker Lewis acid trimethylsilyl trifluoromethanesulfonate (TMSOTf) in this case, and two products were obtained. Although the existence of the four ring nitrogen atoms might have posed regiochemical problems, only N8 regioisomers were obtained, in accordance with their theoretical higher reactivity (in the context of intermediate **4** bearing trimethylsilyl groups) calculated by density functional theory (DFT).[5d] With regard to the anomeric center, α isomers were exclusively formed due to the directing effect of the 1,2-acetyloxonium ion in the course of nucleophilic attack at the C1′ position. The two products were finally identified to be furanoside **1a** and pyranoside **1b**. The coexistence of the five-membered furanoside and six-membered pyranoside has been reported for normal pyrimidine arabinonucleoside synthesis,[10] albeit mainly by spectroscopic characterizations. Such a phenomenon was verified here unambiguously by X-ray analysis of single crystals of compounds **1a** and **1b** obtained from absolute methanol and ethanol, respectively. The nucleobases are planar, adopt the *anti* conformation around the glycosidic bonds (χ(O4′–C1′–N8–C9) = 153.8(3)° for **1a** and χ(O5′–C1′–N8–C9) = 127.1(3)° for **1b**), and located at α positions (Figure 1).

The most striking structural difference resides in their sugar components: **1a** adopts a five-membered furano configuration, whereas **1b** exhibits a six-membered pyrano configuration. The sugar puckering, defined by pseudorotation phase angles (*P*),[11] of **1a** falls into the South range with a C3′-*exo* puckering ($_3T^4$, $P = 212.8(4)°$, $\tau_m = 24.3(3)°$; Figure 1a), which slightly deviates from the common C2′-*endo* puckering for other O- or N-glycosides of arabinofuranose.[12] For **1b**, the six-membered pyranose ring adopts a perfect chair conformation with the nucleobase on the equatorial position. The ramifications of the distinct configurations and conformations are the rather different spatial arrangements of the substituents in each case. The acetoxy groups stemming from the C2′, C3′, and C5′ positions of **1a** stretch parallel to the base plane (Figure 1; Figure S2a and b in the Supporting Information), and the 3′-acetoxy group is opposed to the 5′-acetoxy group with a torsion angle of δ(C5′–C4′–C3′–O3′) = 148.3(6)° (Figure S2b in the Supporting Information), similar to that between the 3′-OH and 5′-OH groups of natural B-DNA (156°), which direct the orientation of the sugar–phosphate backbone. However, for **1b**, the 5′-OH group participated in aminal formation with the 4′-acetoxy group on the sugar ring instead. The 2′-acetoxy group of **1b** stretches along a direction almost perpendicular to the base plane, and there is a bending relationship between the 3′- and 4′-acetoxy groups (δ(O4′–C4′–C3′–O3′) = −50.4(9)°; Figure S2d–f in the Supporting Information).

© 2014 Wiley-VCH Verlag GmbH & Co. KGaA, Weinheim

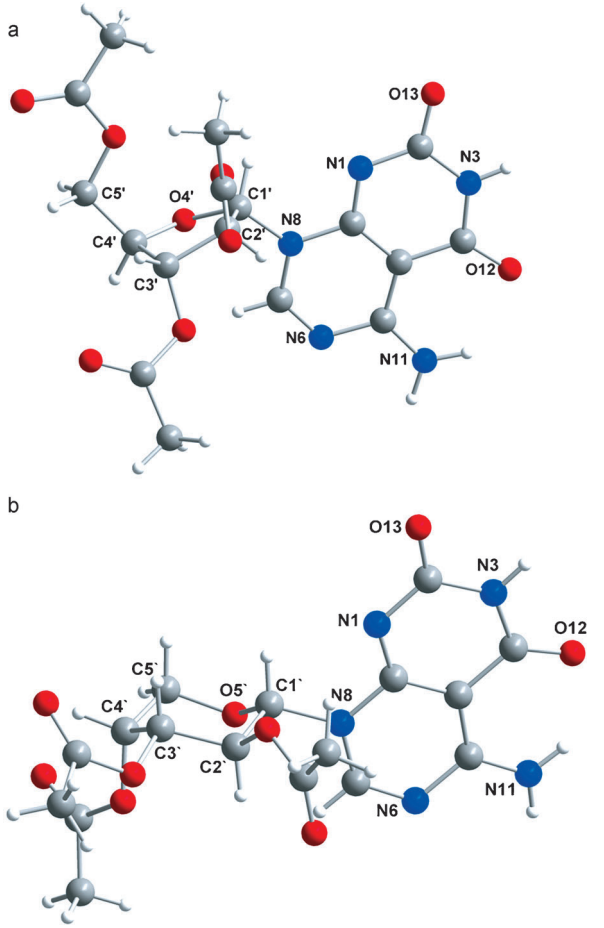

Figure 1. Structures of the monomeric nucleosides. a) Compound **1a** with a sugar moiety with the furanosyl configuration and S-type (C3′-*exo*) sugar puckering. b) Compound **1b** with a sugar moiety with the pyranosyl configuration and chair conformation. Atoms are color coded as follows: red: oxygen; blue: nitrogen; gray: carbon; white: hydrogen.

Overall supramolecular structures in the solid state

The spatial orientations of the sugar substituents have profound effects on the overall supramolecular solid state. For **1a**, along the paper plane direction, the adjacent base moieties are joined head-to-head and the sugar residues are joined tail-to-tail (Figure 2a). Together, these act as noncovalent synthons to construct an infinite stepwise linear extension with a step height of 5.3 Å and a step length of 23.0 Å. Accordingly, zigzag channels with a width of 3.7 Å were formed between these neighboring layers. Perpendicular to the paper plane direction (Figure 2b), the individual monomers are also joined in a side-by-side manner to form a straight infinite linear extension of base tapes and rectangular channels encircled by sugars. Overall, a well-organized noncovalently cross-linked 3D network with linear extension in two directions is produced. For **1b**, along the paper plane direction (Figure 2c), although the sugar residues were still joined tail-to-tail, the adjacent base moieties were blocked to form head-to-head base pairs, which was caused by the perpendicular relationship between the 2′-acetoxy group and the base moiety. Thus, the infinite linear extension of base pairs is terminated along this direction. In the vertical direction, the base moieties still formed a side-by-side arrangement wrapped in channels composed of sugar walls (Figure 2d). There were no head-to-head connection between the bases, so the width of the vertical linear base tape of **1b** (4.2 Å) is narrower than that of **1a** (12.3 Å), and the lower number of base pairs in **1b** will naturally lead to overall weaker interactions along this linear tape compared with those in **1a**.

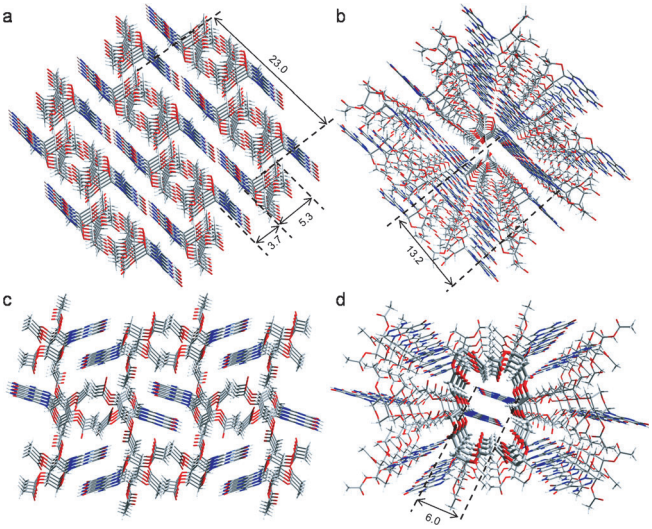

Figure 2. Different views of the overall supramolecular assemblies of compounds **1a** and **1b**. a) Side view of the **1a** solid superstructure showing the infinite stepwise linear extension and zigzag channels. b) Perspective view of the **1a** solid superstructure showing the infinite base tapes and sugar channels perpendicular to the paper plane direction. c) A portion of the 3D network structure of compound **1b** showing the blocked base-pair extension along the paper plane direction. d) Perspective view of the **1b** assembly showing the stacked base tapes and channels along the direction perpendicular to the paper plane, with the central channel highlighted with bolder bond radii. H bonds are not shown for clarity. The unit-to-unit distances shown are in Å. Atoms are color coded as in Figure 1.

Details of base pairs

By looking closer, one can see drastically distinct detailed hydrogen-bond connectivities of the base pairs of **1a** and **1b** (Figure 3). Although many base-pair motifs (of canonical or artificial pyrimidines or purines) have been investigated,[2g,11] the base-pair patterns of the pyrimido[4,5-d]pyrimidine nucleosides have not been explored systematically up to now due to the limited compound numbers. Initially, we supposed **1a** and **1b** may form either Watson–Crick or reverse Watson–Crick base pairs based on the rationale that they have only Watson–Crick faces (Figure S1 in the Supporting Information) and no real Hoogsteen faces and based on the previous experimental evidence that reverse Watson–Crick base pairs were exclusively adopted by several J-AT ribonucleoside derivatives.[5b,f] Surprisingly, neither **1a** nor **1b** adopted the expected base-pair motifs and they were also different from each other.

For **1a**, two types of base arrangement coexist: head-to-head and side-by-side (Figure 3a). The head-to-head base pair is connected through two symmetric hydrogen bonds (N11–

© 2014 Wiley-VCH Verlag GmbH & Co. KGaA, Weinheim

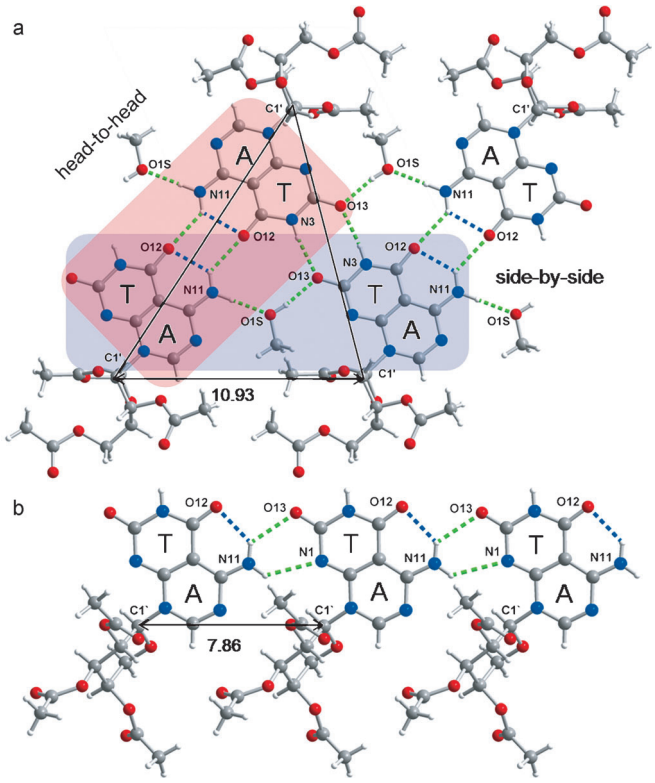

Figure 3. Two distinct base-pair motifs. a) A detailed view of the unusual base pairs in the solid state of **1a**; the head-to-head and side-by-side arrangements are highlighted with red and purple shading, respectively, and the repeated triplet unit is represented with a triangle. b) The base-pair pattern of **1b**. H bonds are shown with dashed lines. The repeated intermolecular hydrogen bonds connecting adjacent molecules are highlighted in green; the intramolecular hydrogen bonds are highlighted in blue. The unit-to-unit distances shown are in Å. Atoms are color coded as in Figure 1.

H11A···O12) between adjacent opposing molecules (like a base pair of DNA between two opposite strands), in which the N11–H11A moiety forms a donating bifurcated geometry (with an intramolecular hydrogen bond). As a whole, a rectangular hydrogen-bond arrangement is formed here by two intermolecular and two intramolecular hydrogen bonds. So, this part is also capable of forming base pairs like the Hoogsteen face of adenine.[13] The exocyclic carbonyl group (O12 atom from the thymine ring) can also act as an acceptor group in lieu of the N7 atom of adenine, so this face can be taken as, in fact, a quasi-Hoogsteen face (the detailed geometry parameters are compared in Figure S3 in the Supporting Information). The side-by-side base pair is actually connected by one base, through a methanol molecule bridge (N11–H11B···O1S, O1S–H4S···O13), with the neighboring base. More interestingly, within this neighboring base, the O13 and N3 atoms form additional two intermolecular hydrogen bonds (N3–H1···O13) with the aforementioned opposite base through the Watson–Crick face, which results in a symmetric homopyrimidine T–T base pair, rather than a Watson–Crick A–T base pair. In general, a coplanar triplet unit is formed, the repeating of which results in an infinite linear base tape in this direction. Triplets are interesting structures involved in triplex-forming oligonucleotides, which have potential for gene inhibition, activation, and therapy.[14]

Compound **1b** (Figure 3b) adopts a different base-pair pattern, which has only side-by-side relationships. This unusual base pair is formed through a bifurcated hydrogen bond between the amino group of the adenine ring with the C2 carbonyl function (O13) and the ring nitrogen atom (N1) of the thymine ring (N11–H11A···O13 and N11–H11B···N1), which is located on neither a Watson–Crick nor a quasi-Hoogsteen face. Such an interaction involving the N1 atom of the thymine ring has never been found before because (in the pyrimidine series) it is always occupied by the sugar residue and not available as a hydrogen-bond acceptor. These two intermolecular hydrogen bonds form the repeated unit by connecting adjacent nucleobases side by side to form an infinite one-dimensional tape with π–π stacking between upper and lower layers (Figure 2d; Figure S4 in the Supporting Information) in an opposite manner.

Details of sugar–sugar connections

The sugar–sugar arrangements are also quite different between **1a** and **1b**. For **1a** (Figure 4a), the sugar residues form an infinite tandem zigzag linear arrangement with an alternating reversed orientation of the pentofuranose ring and protruding bases on the outside (reminiscent of Pauling and Corey's unfortunate DNA model with a central sugar backbone and radially projecting bases[15]). In this linear arrangement, three adjacent sugar residues are held together as the repeated unit with two types of van der Waals contacts: 1) Contacts between the 2′- and 3′-acetyl groups with atomic distances of 4.30 and 3.91 Å for C21′–C31′ and C22′–C32′, respectively; in this case, two symmetrical 2′- and 3′-acetyl contacts together with the upper and lower bases formed a noncovalently enclosed cavity (Figure 4a1); and 2) contacts between 3′-acetyl groups and C4′–C5′ bonds with atomic distances of 4.28 and 3.75 Å for C31′–C4′ and C32′–C5′, respectively (Figure 4a2). In the case of compound **1b** (Figure 4b), the bending relationship between the 3′- and 4′-acetoxy groups instead leads to the formation of two channels. The bigger one, trapping two stacked base tapes, is formed by C–H···O type weak hydrogen bonds of the 2′-acetyl group with the 5′-methylene group (C5′–5′···O21′; Figure 4b1; Figure S5b in the Supporting Information). This wrapped channel structure is enforced by two hydrogen bonds connecting the base and sugar together (N3–H3···O5′ and C5′–H5′B···O13; Figures S4 and S5 in the Supporting Information). The smaller channel was formed by C–H···O type weak hydrogen bonds of C5′–H5′···O21′ and C32′–H32B···O41′ (Figure 4b2; Figure S5c in the Supporting Information).

Gelation of compound 1a

One of the crucial differences between these two compounds is that the base tape of **1a** consisted of more hydrogen bonds (and was thus more stable than that of **1b**) and extends in crossing directions in space. To see if these microscopic fea-

© 2014 Wiley-VCH Verlag GmbH & Co. KGaA, Weinheim

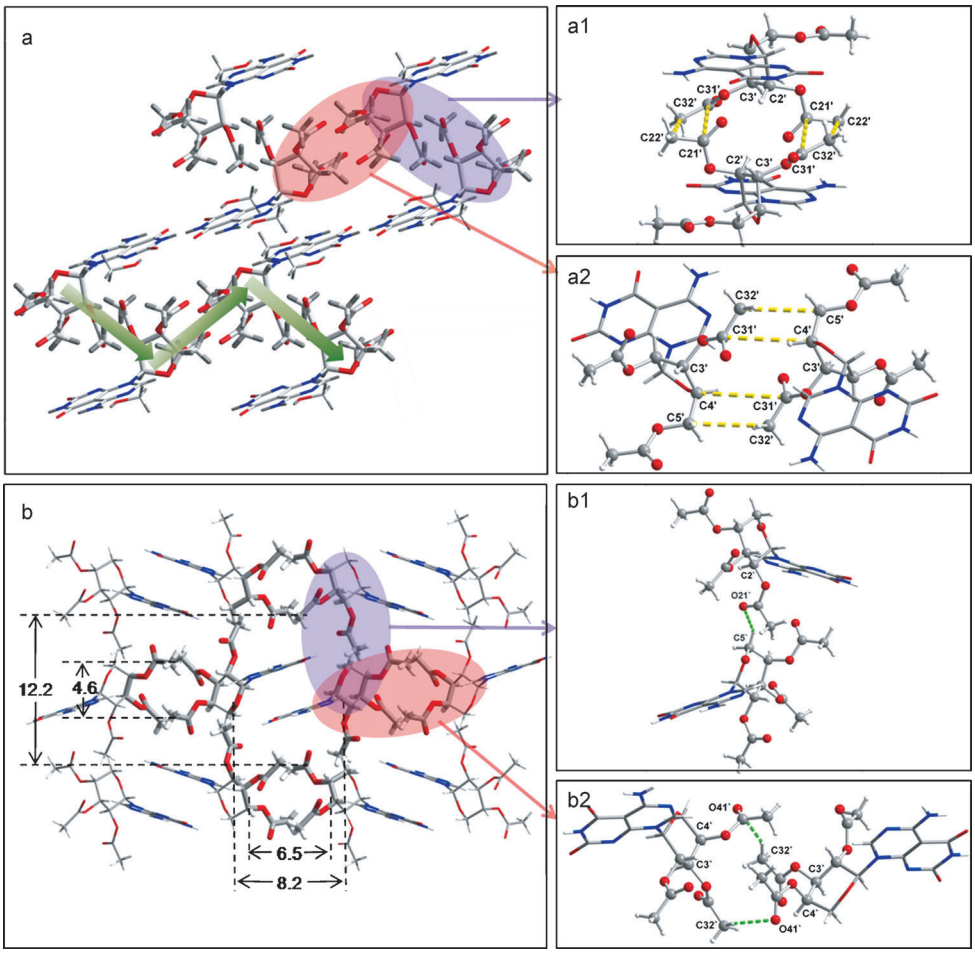

Figure 4. Different sugar–sugar arrangements in the **1a** and **1b** self-assemblies. a) The infinite tandem zigzag linear sugar arrangement in the **1a** assembly, highlighted with bolder bond radii and represented with green arrows, consisted of a repeated three-molecule unit with two types of intermolecular van der Waals contacts, which are highlighted with red and purple ovals, respectively. a1) A detailed view of the symmetrical van der Waals contacts between the 2′- and 3′-acetyl groups from adjacent sugar residues of **1a** and the resultant cavity structure. a2) A detailed view of the symmetrical van der Waals contacts between the 3′-acetyl group and the C4′–C5′ bond from adjacent sugar residues of **1a**. b) The bending of the substituent groups on the sugar rings of **1b** constitutes two types of channels, which are highlighted with bolder bond radii. b1) A detailed view of the interactions between the 2′-acetyl group and 5′-methylene group from adjacent **1b** molecules. b2) A detailed view of the interactions between the 3′- and 4′-acetoxy groups from adjacent **1b** molecules. The van der Waals contacts of interest are highlighted in yellow; the intermolecular hydrogen bonds are highlighted in green. The unit-to-unit distances shown are in Å. Atoms are color coded as in Figure 1.

tures were able to be translated into macroscopic properties, the gelation behaviors of compounds **1a** and **1b** were investigated in 20 different organic solvents. Low-molecular-weight gelators have drawn much attention recently for building nanoscale soft materials due to the well-defined and fine-tunable chemical structures of their discrete molecular components. The prerequisite for gelation is the spontaneous self-assembly of small molecules into entangled fibrous structures resulting from molecular-level recognition.[16] From this perspective, **1a** could act as an organogelator by its cross-linked infinite linear tapes and **1b** may not gelate solvent because one of its linear structures is truncated (Figure 2c). As expected (Table S1 in the Supporting Information), **1b** could not gelate any of the investigated solvents, whereas **1a** acted as a very strong gelator in chloroalkanes, with similar microscopic xerogel morphologies (Figure 5; Figures S6–S9 in the Supporting Information). The critical gelation concentration of **1a** was rather low: 0.4–0.6 wt% in 1, 2-dichloroethane, dichloromethane, and chloroform, which indicates that **1a** falls into the range of supergelators.[17] At a concentration of 1 wt%, the **1a**/1,2-dichloroethane system formed a rather robust gel with a sol–gel transition temperature (T_{gel}) of 91 °C, which is higher than the boiling point of the solvent itself (83 °C). The mechanical properties of the gels of compound **1a** were characterized by rheological measurements; dynamic strain sweep and oscillatory frequency sweep experiments confirmed their typical viscoelastic natures (Figure S10 in the Supporting Information). The solvent selectivity of **1a** was analyzed by correlating gelation abilities with Hildebrand (δ) and Hansen (δ_d, δ_p, δ_h) parameters[18] (Table S2 in the Supporting Information). A narrow favorable δ_h domain (δ_h accounts for hydrogen-bonding interactions) for gelation was established (Figure S11 in the Supporting Information), which indicated that the self-assembly of **1a** is hydrogen-bond-interaction dependent, in accordance with the information obtained from the crystal structure. On the basis that J-AT has the potential to base pair with adenine and thymine/uracil in competition with its self-complementary association, the molecular recognition of the **1a** organogel was also investigated through titration experiments. The results indeed supported the capability of **1a** to base pair with adenine or uracil derivatives (Table S3 in the Supporting Information), because the addition of guanine or cytosine derivatives did not influence the gel stability within the saturated concentrations whereas addition of adenine or thymine derivatives destabilized the gel system.

Supramolecular self-assemblies of compounds 2a and 2b in the solution state

Supramolecular morphogenesis is a fundamentally important process in a variety of fields ranging from structural biology to

© 2014 Wiley-VCH Verlag GmbH & Co. KGaA, Weinheim

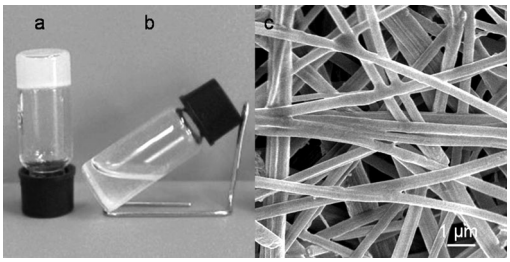

Figure 5. Gelation experiments: a) **1a** in 1,2-dichloroethane (1 wt%) formed a robust gel; b) **1b** in 1,2-dichloroethane (1 wt%) did not undergo gelation. c) SEM image of the **1a** xerogel prepared in 1,2-dichloroethane.

material chemistry. Previously, the mechanistic process of the formation of the flower-shaped superstructures has been addressed in detail for free J-AT ribonucleosides in water, and the central role of the 2′-OH group has been established.[5f] By closer inspection of the molecular structures of the J-AT ribo- and arabinonucleosides (Figure S13 in the Supporting Information), one can see the sugar configurations of them, and the relative spatial relationship between the base moiety and the 2′-OH group is the same (just with the opposite direction around the the C1′–C2′ bond). Therefore, it is very interesting and necessary to investigate whether the same complex supramolecular morphology will still be reproduced by the corresponding J-AT arabinonucleosides. The free nucleosides **2a** and **2b** were obtained by treatment of **1a** and **1b** with 0.2 M sodium methoxide. The unmasking of the hydroxy groups made them more water soluble, and consequently, the morphologies of the supramolecular assemblies in solution state were investigated. Compound **2a** indeed formed flower-shaped superstructures in aqueous solution, with uniform diameters of approximate 20 μm and the petal thicknesses of about 80 nm (Figure S12 in the Supporting Information), which gave us further experimental evidence for our earlier observations and conclusions. In addition, apart from the general similarity with the flower of the J-AT ribonucleoside, a subtle difference between them should be noticed: the petals of the microflower of **2a** were cross-linked with each other, whereas those of the ribonucleosides were discrete (Figure S13 in the Supporting Information). This difference might indicate the effects of the spatial arrangement of the 3′-OH and 5′-OH groups in both cases. In comparison, **2b** under the same conditions could not form the flower-shaped morphology, which indicated the influence of the six-membered configuration. It formed microspheres instead, with average diameters of about 25 μm and with a porous structured surface consisting of interweaved nanobundles. Of course, the high-resolution elucidation of the atomic connectivities for the morphological differences between compounds **2a** and **2b** and the J-AT ribonucleosidea currently remains a challenge because crystals of the free nucleosides suitable for X-ray structure determination have not yet been obtained.

Conclusions

In parallel with natural selection, the chemical evolution of nucleosides in chemists' hands has not seen its end yet, and novel structures obtained through a myriad of modifications always lead to the emergence of new properties. We have found that a new type of J-AT ribonuleosides can form complex-shaped superstructures. It is of great interest to investigate the relationship between their microscopic and macroscopic structures systematically. For this purpose, the corresponding pyrimido[4,5-d]pyrimidine arabinonucleosides were synthesized, and some new phenomena were found. The first striking difference was the coexistence of furanosyl and pyranosyl sugar configurations. The configuration determined the spatial arrangement of the substituents, which in turn exhibited restrictions on the base-pair patterns; consequently, two novel base-pair motifs (through a quasi-Hoogsteen face or the N1 atom of the thymine ring) were adopted by the furanosyl or pyranosyl nucleosides. These unique orchestrating interactions led to the formation of certain higher structures: two elaborate supramolecular solids containing hollow channels and cavities and the robust organogels formed by compound **1a**. In addition, the two free nucleosides also formed morphologically different self-assemblies in the solution state. Evidently, the microscopic interactions (the chemical information stored in the hydrogen-bonding patterns) were translated into the higher structures at different levels.

Initially, by following the concept of two-faced, Janus type guanine–cytosine derivatives,[4a] we synthesized the corresponding ribonucleosides of J-GC and J-AT and supposed that they would form self-complementary base pairs dominantly through Watson–Crick faces. However, on closer inspection, we see that, apart from the Watson–Crick faces, the A–T pyrimido-[4,5-d]pyrimidine does have two more faces with hydrogen-bonding capabilities that could easily escape notice: the quasi-Hoogsteen face and the N1 atom of the thymine ring. From this point, the A–T pyrimido[4,5-d]pyrimidine base is more than just a Janus type molecule. More importantly, how the programmed hydrogen-bonding information of this nucleobase is read turns out to be tailored by the sugar counterparts. Selective noncovalent hydrogen bonds in complementary base paring are the basis of the genetic information flows in DNA replication, in RNA transcription, or between codon and anticodon in protein translation. It was proposed that the four canonical nucleobases (the primary information layer) alone are neither sufficient for the complex functions of RNA nor sufficient for the encoding of heritable genetic information in DNA, and the numerous noncanonical nucleobases that exist in them (as a secondary information layer) play indispensible roles, especially for the functions of RNA.[19] Up to now, most of the research on the expression of the specific hydrogen-bonding information has focused on only the nucleobases themselves. The research into how the interplay between the sugar counterparts and the base moieties influences the readout of the hydrogen-bonding pattern information is generally overlooked. Now that we have found that the sugar can direct the same base to form completely different base pairs and can

© 2014 Wiley-VCH Verlag GmbH & Co. KGaA, Weinheim

even lead to the formation of completely distinct higher structures, this prompts us to raise an interesting conjecture: is the expression of genetic information in the complex biological context also influenced (under certain circumstances, through internal or external factors) by orchestrating between the sugar backbone (through certain modification or even the existence of noncanonical sugar configurations) and the base sequence? Further investigation on this question might produce some interesting findings about whether or not there exists a third layer of information in RNA or DNA.

Finally, besides the theoretical interest, the novel base pairs formed by **1a** and **1b** indicate their potential applications to serve as new synthons and molecular tectons to widen the complex matters in supramoleular chemistry[20] through the high malleability of the hydrogen-bonding patterns. In addition, the regular cavities/channels featured in the solid-state structures of **1a** and **1b**, in which specific-sized and -shaped guest species might reside, suggests that they could act as efficient solid-state host–guest clathrates for molecule sensing, pharmacological usages, or template-synthesis purposes.[21] The recognition of these new-type nucleosides with neutral guest molecules in the solid state and the specific interactions with charged ions in the solution state are currently under investigation.

Experimental Section

General

All chemicals were commercially available. The solvents and reagents were analytically pure. The solvents 1, 2-dichloroethane and acetonitrile were purified by distillation from P_2O_5. Thin-layer chromatography (TLC) was performed on aluminum sheets covered with silica gel 60 F254 (0.2 mm, Merck, Germany). Flash column chromatography (FC) was carried out with silica gel 60 (Haiyang chemical company, P. R. China) at 0.4 bar. NMR spectra were recorded on a Bruker AV II spectrometer (Bruker, Germany) at 400 MHz and 600 MHz; the chemical shift (δ) values in ppm are relative to Me_4Si as the internal standard. High-resolution mass spectra were measured with a mass analyzer (Q-TOF, Bruker, Germany). The UV absorption spectra were recorded on a DU-800 spectrophotometer (Beckman, US.

Gelation tests

Compound **1a/1b** (5 mg) was added to a screw-capped glass sampler vial, to which solvent (100 μL) was added in one portion. The vial was heated to promote the dissolution of the mixture. The solution was then gradually allowed to cool to room temperature to see if a gel was formed. If the sample was insoluble at the boiling point of the solvent, solvent (100 μL each time) was added until the total volume reached 1000 μL. Gelation was considered to have occurred if a homogeneous substance that exhibited no gravitational flow was obtained. The sol–gel transition temperature (T_{gel}) was assumed to be the temperature at which the gel started to flow if the sealed vial containing the gel was immersed inversely in a thermostatted oil bath with the temperature rising at a rate of 1 °C min^{-1}.

Rheological studies

Rheological studies were carried out with a stress-controlled rheometer (TA Instruments, AR 2000ex) equipped with steel parallel-plate geometry (20 mm diameter). The gap distance was fixed at 0.025 mm. The gel was scooped onto the plate of the rheometer. Strain sweep at a constant frequency (6.28 rad s^{-1}) was performed in the 0.01–100% range to determine the linear viscoelastic region (LVR) of the gel sample. Oscillatory frequency sweep was obtained at 0.1–100 rad s^{-1} at a constant strain of 0.1%, well within the linear regime determined by the strain sweep, to ensure that the calculated parameters corresponded to an intact network structure. All measurements were carried out at a constant temperature (20 °C). The rheometer had a built-in computer and the US-200 software converted the torque measurements into the storage modulus (G′) and loss modulus (G″) values.

SEM imaging of xerogels

Gels (2 wt%) of compound **1a** were freeze-dried with an EYEL4 FDU-2100 freezing drier for 24 h. The resulting xerogel samples were fractured and coated with gold. The surface morphology was observed with a JSM-7500F instrument.

SEM imaging of aqueous solutions

SEM imaging of the supramolecular self-assemblies of **2a** and **2b** in water was performed with a high-resolution INSPECT F50 instrument. All SEM images were obtained without staining. Samples were prepared by dissolving the appropriate compounds in H_2O (0.2 mg mL^{-1}), heating the solutions to 100 °C, and then allowing them to cool to room temperature for 48 h.

Crystallographic study

X-ray-quality colorless crystals of **1a** and **1b** were obtained by slow evaporation from absolute ethanol and methanol, respectively. Proper-sized single crystals were stabilized into a tiny glass tube including mother liquor with epoxy resin to minimize solvent loss. Crystal data were collected at 296 K on a Bruker Apex II instrument. CCDC 997732 (**1a**) and 940971 (**1b**) contain the supplementary crystallographic data for this paper. These data can be obtained free of charge from the Cambridge Crystallographic Data Centre via www.ccdc.cam.ac.uk/data_request/cif.

Crystal data for **1a**: $C_{18}H_{23}N_5O_{10}$; formula weight: 469.41; triclinic; $P\bar{1}$; $a=10.3546(9)$, $b=10.7846(9)$, $c=10.9259(1)$ Å; $\alpha=64.985(5)$, $\beta=89.469(6)$, $\gamma=79.184(6)^\circ$; $V=1082.64(16)$ Å^3; $Z=2$; $D_x=1.461$ g cm^{-3}; $\mu=0.126$ mm^{-1}; $R_{int}=0.0340$; GOF = 1.073; $R_1=0.0554$; $wR_2=0.1327$ for 2614 data with $I>2\sigma(I)$.

Crystal data for **1b**: $C_{17}H_{19}N_5O_9$; formula weight: 437.37; orthorhombic; $P2_12_12$; $a=15.183(2)$, $b=16.916(2)$, $c=7.8583(1)$ Å; $\alpha=90$, $\beta=90$, $\gamma=90^\circ$; $V=2018.3(5)$ Å^3; $Z=4$; $D_x=1.439$ g cm^{-3}; $\mu=0.118$ mm^{-1}; $R_{int}=0.0231$; GOF = 1.041; $R_1=0.0336$; $wR_2=0.0855$ for 3750 data with $I>2\sigma(I)$.

2,3,5-Tri-*O*-acetyl-D-arabinose (6)

NaOAc (2.0 g, 24 mmol) was suspended in Ac_2O (30 mL), and the mixture was heated to reflux at 110 °C for about 3 min. D-(−)-Arabinose (**5**; 5.0 g, 33 mmol) was then added in portions. After 10 min, the reaction was accomplished (as monitored by TLC). The mixture was then poured into ice water (300 mL) and neutralized by addition of solid $NaHCO_3$. The mixture was extracted with CH_2Cl_2 (3× 120 mL). The combined organic phases were dried and concentrat-

© 2014 Wiley-VCH Verlag GmbH & Co. KGaA, Weinheim

ed. The residue was then purified by FC to afford a colorless syrup (10.0 g, 96%). HRMS (ESI+): *m/z* calcd for $C_{13}H_{18}O_9$: 341.0849 $[M+Na]^+$; found: 341.0850.

5-Amino-8-(2,3,5-tri-*O*-acetyl-α-D-arabinofuranosyl)pyrimido-[4,5-d]pyrimidine-2,4-(3*H*,8*H*)-dione (1a) and 5-amino-8-(2,3,5-tri-*O*-acetyl-α-D-arabinopyranosyl)pyrimido[4,5-d]pyrimidine-2,4-(3*H*,8*H*)-dione (1b)

Compound **3** (2.0 g, 11.2 mmol) was suspended in hexamethyldisilazane (HMDS) (150 mL), and the mixture was stirred at 140 °C for about 3 min. Trimethylsilyl chloride (TMSCl) (2 mL, 15.8 mmol) was then added, and the reaction was stirred with heating at reflux until the mixture was clear. After evaporation of the solution to remove the HMDS, the resulting silylated base, **4**, was dissolved in dry 1,2-dichloroethane (60 mL), to which the syrup of tetraacetylated D-arabinose (**6**; 1.8 g, 5.7 mmol) suspended in dry acetonitrile (60 mL) was added. $SnCl_4$ (1.8 mL, 13.6 mmol) was added as the catalyst at 0 °C. After the mist vanished, the reaction flask was moved to an oil bath and stirred at 80 °C with exclusion of moisture. After 3 h, saturated $NaHCO_3$ aqueous solution (120 mL) was added at 0 °C to quench the reaction; CH_2Cl_2 (3×120 mL) was used to extract the organic phase. After being dried with anhydrous Na_2SO_4, the organic phase was evaporated. The residue was applied to FC (CH_2Cl_2:isopropanol, 98:2) to furnish compounds **1a** (1370 mg, 28%) and **1b** (1220 mg, 25%).

Compound **1a**: UV (MeOH): λ_{max} (ε) = 233 (17000), 250 (30000), 277 nm (7200 $dm^3 mol^{-1} cm^{-1}$); ^1H NMR (400 MHz, [D$_6$]DMSO): δ = 1.86 (3H, s, OAc), 1.99 (3H, s, OAc), 2.20 (3H, s, OAc), 4.03–4.07 (1H, dd, J_1 = 13.1 Hz, J_2 = 1.7 Hz, 5′-H$_a$), 4.21–4.25 (1H, d, J = 13.2 Hz, 5′-H$_b$), 5.25–5.35 (2H, m, 4′-H and 3′-H), 5.51–5.55 (1H, dd, J_1 = 10.0 Hz, J_2 = 3.3 Hz, 2′-H), 6.48–6.51 (1H, d, J = 8.8 Hz, 1′-H), 8.57 (1H, s, CH), 9.14–9.15 (1H, d, J = 3.3 Hz, NH$_\alpha$), 9.21–9.22 (1H, d, J = 3.2 Hz, NH$_\beta$), 10.84 ppm (1H, s, NH); ^{13}C NMR (150 MHz, [D$_6$]DMSO): δ = 20.43, 20.86, 21.11, 67.02, 68.19, 69.50, 70.31, 79.91, 86.67, 152.26, 156.81, 157.69, 161.48, 165.32, 169.86, 170.29, 170.50 ppm; HRMS (ESI+): *m/z* calcd for $C_{17}H_{19}N_5O_9$: 460.1081 $[M+Na]^+$; found: 460.1080.

Compound **1b**: UV (MeOH): λ_{max} (ε) = 250 (31000), 277 nm (7300 $dm^3 mol^{-1} cm^{-1}$); ^1H NMR (400 MHz, [D$_6$]DMSO): δ = 2.01 (3H, s, OAc), 2.07 (3H, s, OAc), 2.11 (3H, s, OAc), 4.16–4.20 (1H, dd, J_1 = 12.1 Hz, J_2 = 6.4 Hz, 5′-H$_a$), 4.32–4.36 (1H, dd, J_1 = 12.1 Hz, J_2 = 4.1 Hz, 5′-H$_b$), 4.98–5.02 (1H, m, 4′-H), 5.26–5.28 (1H, m, 3′-H), 5.66–5.67 (1H, t, J = 3.3 Hz, 2′-H), 6.29 (1H, d, J = 3.0 Hz, 1′-H), 8.55 (1H, s, CH), 9.01 (1H, d, J = 3.5 Hz, NH$_\alpha$), 9.07 (1H, d, J = 3.5 Hz, NH$_\beta$), 10.81 ppm (1H, s, NH); ^{13}C NMR (150 MHz, [D$_6$]DMSO): δ = 20.99, 21.04, 25.93, 63.35, 75.24, 78.82, 83.01, 87.49, 91.19, 152.03, 156.69, 157.83, 162.06, 165.28, 169.88, 169.90, 170.58 ppm; HRMS (ESI+): *m/z* calcd for $C_{17}H_{19}N_5O_9$: 460.1081 $[M+Na]^+$; found: 460.1079.

5-Amino-8-(α-D-arabinofuranosyl)pyrimido[4,5-d]pyrimidine-2,4-(3*H*,8*H*)-dione (2a)

Compound **1a** (180 mg, 0.4 mmol) was suspended in 0.2 M NaOMe/MeOH (12 mL), and the mixture was heated to reflux at 70 °C for about 1 h. After cooling to room temperature, the solution was neutralized with diluted acetic acid to pH 6.5, and a precipitate formed. After filtration, the precipitate was washed with methanol (3×5 mL) and water (1×5 mL). The target compound **2a** was obtained as a white powder by vacuum drying (90 mg, 72%). UV (MeOH): λ_{max} (ε) = 232 (9400), 251 (16000), 277 nm (5300 $dm^3 mol^{-1} cm^{-1}$); ^1H NMR (600 MHz, [D$_6$]DMSO): δ = 3.55–3.58 (1H, m, 4′-H), 3.70–3.72 (2H, d, J = 12.4 Hz, 5′-H$_2$), 3.82–3.84 (1H, d, J = 11.1 Hz, 3′-H), 3.88–3.92 (1H, m, 2′-H), 4.74–4.75 (1H, d, J = 6.6 Hz, OH), 5.03–5.04 (1H, d, J = 5.5 Hz, OH), 5.36–5.37 (1H, d, J = 5.2 Hz, OH), 5.88–5.89 (1H, d, J = 9.4 Hz, 1′-H), 8.55 (1H, s, CH), 9.11 (2H, s, NH$_2$), 10.81 ppm (1H, s, NH); ^{13}C NMR (150 MHz, [D$_6$]DMSO): δ = 69.04, 69.67, 70.41, 73.65, 83.25, 87.19, 152.81, 157.01, 158.29, 161.77, 165.49 ppm; HRMS (ESI+): *m/z* calcd for $C_{11}H_{13}N_5O_6$: 334.0764 $[M+Na]^+$; found: 334.0765.

5-Amino-8-(α-D-arabinopyranosyl)pyrimido[4,5-d]pyrimidine-2,4-(3*H*,8*H*)-dione (2b)

Compound **1b** (130 mg, 0.3 mmol) was suspended in 0.2 M NaOMe/MeOH (9 mL), and the mixture was heated to reflux at 70 °C for about 30 min. After cooling to room temperature, the solution was neutralized with diluted acetic acid to pH 6.5, and a precipitate formed. The precipitate was filtered and washed with methanol (3×4 mL) and water (1×3 mL). The target compound **2b** was obtained as a white powder by vacuum drying (65 mg, 70%). UV (MeOH): λ_{max} (ε) = 251 (17000), 277 nm (5600 $dm^3 mol^{-1} cm^{-1}$); ^1H NMR (400 MHz, [D$_6$]DMSO): δ = 3.59–3.60 (2H, d, J = 2.3 Hz, 5′-H$_2$), 3.98–3.99 (1H, d, J = 2.0 Hz, 3′-H), 4.20 (1H, s, 4′-H), 4.36–4.40 (1H, m, 2′-H), 5.11 (1H, s, OH), 5.43–5.44 (1H, d, J = 2.8 Hz, OH), 5.85–5.86 (1H, d, J = 3.3 Hz, OH), 6.07 (1H, d, J = 1.6 Hz, 1′-H), 8.41 (1H, s, CH), 8.92–8.94 (2H, d, J = 7.2 Hz, NH$_2$), 10.79 ppm (1H, s, NH); ^{13}C NMR (150 MHz, [D$_6$]DMSO): δ = 61.85, 76.14, 80.61, 87.46, 90.21, 93.89, 151.69, 157.03, 158.04, 162.16, 165.35 ppm; HRMS (ESI+): *m/z* calcd for $C_{11}H_{13}N_5O_6$: 334.0764 $[M+Na]^+$; found: 334.0766.

Acknowledgements

We thank the National Natural Science Foundations of China (document nos.: 81321002, 20772087, 81061120531, and 30930100), ISTCPC (2012DFA31370), and the Open Foundation (SKLODOF2014OF04) of the State Key Laboratory of Oral Diseases of Sichuan University for the financial support.

Keywords: base pairs · nucleosides · self-assembly · supramolecular chemistry

[1] a) J. D. Watson, F. H. C. Crick, *Nature* **1953**, *171*, 737–738, J. D. Watson, F. H. C. Crick, *Nature* **1953**, *171*, 964–967; b) S. Zamenhof, G. Brawerman, E. Chargaff, *Biochim. Et Biophys. Acta* **1952**, *9*, 402–405; c) M. H. F. Wilkins, A. R. Stokes, H. R. Wilson, *Nature* **1953**, *171*, 738–740; d) R. E. Franklin, R. G. Gosling, *Nature* **1953**, *171*, 740–741.

[2] a) V. B. Pinheiro, A. I. Taylor, C. Cozens, M. Abramov, M. Renders, S. Zhang, J. C. Chaput, J. Wengel, S.-Y. Peak-Chew, S. H. McLaughlin, P. Herdewijn, P. Holliger, *Science* **2012**, *336*, 341–344; b) A. Eschenmoser, *Angew. Chem.* **2011**, *123*, 12618–12681; *Angew. Chem. Int. Ed.* **2011**, *50*, 12412–12472; c) M. Egli, P. S. Pallan, R. Pattanayek, C. J. Wilds, P. Lubini, G. Minasov, M. Dobler, C. J. Leumann, A. Eschenmoser, *J. Am. Chem. Soc.* **2006**, *128*, 10847–10856; d) K.-U. Schöning, P. Scholz, S. Guntha, X. Wu, R. Krishnamurthy, A. Eschenmoser, *Science* **2000**, *290*, 1347–1351; e) M. Beier, F. Reck, T. Wagner, R. Krishnamurthy, A. Eschenmoser, *Science* **1999**, *283*, 699–703; f) A. Eschenmoser, *Science* **1999**, *284*, 2118–21243; g) I. Hirao, M. Kimoto, R. Yamashige, *Acc. Chem. Res.* **2012**, *45*, 2055–2065; h) L. Li, M. Degardin, T. Lavergne, D. A. Malyshev, K. Dhami, P. Ordoukhanian, F. E. Romesberg, *J. Am. Chem. Soc.* **2014**, *136*, 826–829; i) Z. Yang, F. Chen, J. B. Alvarado, S. A. Benner, *J. Am. Chem. Soc.* **2011**, *133*, 15105–15112.

[3] L. P. Jordheim, D. Durantel, F. Zoulim, C. Dumontet, *Nat. Rev. Drug Discovery* **2013**, *12*, 447–464.

[4] a) A. Marsh, M. Silvestri, J.-M. Lehn, *Chem. Commun.* **1996**, 1527–1528; b) M. Mascal, N. M. Hext, R. Warmuth, M. H. Moore, J. P. Turkenburg,

 © 2014 Wiley-VCH Verlag GmbH & Co. KGaA, Weinheim

Angew. Chem. **1996**, *108*, 2348 – 2350; *Angew. Chem. Int. Ed. Engl.* **1996**, *35*, 2204 – 2206; c) F. Seela, T. Wiglenda, H. Rosemeyer, H. Eickmeier, H. Reuter, *Angew. Chem.* **2002**, *114*, 617 – 619; *Angew. Chem. Int. Ed.* **2002**, *41*, 603 – 605; d) J. T. Davis, *Angew. Chem.* **2004**, *116*, 684 – 716; *Angew. Chem. Int. Ed.* **2004**, *43*, 668 – 698; e) J. G. Moralez, J. Raez, H. Fenniri, *J. Am. Chem. Soc.* **2005**, *127*, 8307 – 8309; f) G. Borzsonyi, R. L. Beingessner, T. Yamazaki, J.-Y. Cho, A. J. Myles, M. Malac, R. Egerton, M. Kawasaki, K. Ishizuka, A. Kovalenko, H. Fenniri, *J. Am. Chem. Soc.* **2010**, *132*, 15136 – 15139; g) B. Saccà, C. M. Niemeyer, *Angew. Chem.* **2012**, *124*, 60 – 69; *Angew. Chem. Int. Ed.* **2012**, *51*, 58 – 66; h) W. Liu, H. Zhong, R. Wang, N. C. Seeman, *Angew. Chem.* **2011**, *123*, 278 – 281; *Angew. Chem. Int. Ed.* **2011**, *50*, 264 – 267.

[5] a) H. Z. Yang, M. Y. Pan, D. W. Jiang, Y. He, *Org. Biomol. Chem.* **2011**, *9*, 1516 – 1522; b) M. Pan, W. Hang, X. Zhao, H. Zhao, P. Deng, Z. Xing, Y. Qing, Y. He, *Org. Biomol. Chem.* **2011**, *9*, 5692 – 5702; c) H. Zhao, W. Huang, X. Wu, Z. Xing, Y. He, Q. Chen, *Chem. Commun.* **2012**, *48*, 6097 – 6099; d) H. Zhao, S. He, M. Yang, X. Guo, G. Xin, C. Zhang, L. Ye, L. Chu, Z. Xing, W. Huang, Q. Chen, Y. He, *Chem. Commun.* **2013**, *49*, 3742 – 3744; e) S. He, H. Zhao, X. Guo, G. Xin, B. Huang, L. Ma, X. Zhou, R. Zhang, D. Du, X. Wu, Z. Xing, W. Huang, Q. Chen, Y. He, *Tetrahedron* **2013**, *69*, 9245 – 9251; f) H. Zhao, X. Guo, S. He, X. Zeng, X. Zhou, C. Zhang, J. Hu, X. Wu, Z. Xing, L. Chu, Y. He, Q. Chen, *Nat. Commun.* **2014**, *5*, 3108.

[6] a) M. Ohtawa, S. Ichikawa, Y. Teishikata, M. Fujimuro, H. Yokosawa, A. Matsuda, *J. Med. Chem.* **2007**, *50*, 2007 – 2010; b) M. Johar, T. Manning, C. Tse, N. Desroches, B. Agrawal, D. Y. Kunimoto, R. Kumar, *J. Med. Chem.* **2007**, *50*, 3696 – 3705; c) A. Schweifer, F. Hammerschmidt, *J. Org. Chem.* **2011**, *76*, 8159 – 8167; d) O. Jungmann, M. Beier, A. Luther, H. K. Huynh, M. O. Ebert, B. Jaun, R. Krishnamurthy, A. Eschenmoser, *Helv. Chim. Acta* **2003**, *86*, 1259 – 1308; e) W. A. Cristofoli, L. I. Wiebe, E. De Clercq, G. Andrei, R. Snoeck, J. Balzarini, E. E. Knaus, *J. Med. Chem.* **2007**, *50*, 2851 – 2857; f) R. Sendula, E. Orbán, F. Hudecz, G. Sági, I. Jablonkai, *Nucleosides Nucleotides Nucleic Acids* **2012**, *31*, 482 – 500.

[7] U. Niedballa, H. Vorbrueggen, *J. Org. Chem.* **1974**, *39*, 3654 – 3660.

[8] a) R. B. Cohen, K. C. Tsou, S. H. Rutenburg, A. M. Seligman, *J. Biol. Chem.* **1952**, *195*, 239 – 249; b) Y. Su, J. Xie, Y. Wang, X. Hu, X. Lin, *Eur. J. Med. Chem.* **2010**, *45*, 2713 – 2718.

[9] B. L. Kam, J.-L. Barascut, J.-L. Imbach, *Carbohydr. Res.* **1979**, *69*, 135 – 142.

[10] J. Maity, G. Shakya, S. K. Singh, V. T. Ravikumar, V. S. Parmar, A. K. Prasad, *J. Org. Chem.* **2008**, *73*, 5629 – 5632.

[11] W. Saenger, *Principles of Nucleic Acid Structure*, Springer, New York, **1984**.

[12] a) S. Cros, C. H. Penhoat, S. Pérez, A. Imberty, *Carbohydr. Res.* **1993**, *248*, 81 – 93; b) P. Tollin, H. R. Wilson, D. W. Young, *Acta Crystallogr. Sect. B* **1973**, *29*, 1641 – 1647; c) G. Biswas, A. Banerjee, *Acta Crystallogr. Sect. C* **1987**, *43*, 1731 – 1734; d) G. Biswas, A. Banerjee, *Acta Crystallogr. Sect. C* **1988**, *44*, 853 – 856; e) G. Biswas, Y. Iitaka, A. Bose, A. Banerjee, *Acta Crystallogr. Sect. C* **1988**, *44*, 1269 – 1272; f) D. Jiang, S. Budow, V. Glacon, H. Eickmeier, H. Reuter, Y. He, F. Seela, *Acta Crystallogr. Sect. C* **2010**, *66*, o194 – o197.

[13] K. Hoogsteen, *Acta Crystallogr.* **1963**, *16*, 907 – 916.

[14] a) V. Malnuit, M. Duca, R. Benhida, *Org. Biomol. Chem.* **2011**, *9*, 326 – 336; b) D. P. Arya, *Acc. Chem. Res.* **2011**, *44*, 134 – 146.

[15] a) L. Pauling, R. B. Corey, *Nature* **1953**, *171*, 346 – 346; b) L. Pauling, R. B. Corey, *Proc. Natl. Acad. Sci. USA* **1953**, *39*, 84 – 97.

[16] a) S. S. Babu, V. K. Praveen, A. Ajayaghosh, *Chem. Rev.* **2014**, *114*, 1973 – 2129; b) L. A. Estroff, A. D. Hamilton, *Chem. Rev.* **2004**, *104*, 1201 – 1217.

[17] H. Bouas-Laurent, J.-P. Desvergne, *Molecular Gels: Materials with Self-Assembled Fibrillar Networks* (Eds.: R. G. Weiss, P. Terech), Springer, Dordrecht, **2006**, Chapter 12.

[18] a) J. Branderup, E. H. Immergut, E. A. Grulke, *Polymer Handbook*, 4edth edWiley, New York, **1999**, pp. 677 – 701; b) M. Raynal, L. Bouteiller, *Chem. Commun.* **2011**, *47*, 8271 – 8273; c) P. Curcio, F. Allix, G. Pickaert, B. Jamart-Grégoire, *Chem. Eur. J.* **2011**, *17*, 13603 – 13612; d) J. Gao, S. Wu, M. A. Rogers, *J. Mater. Chem.* **2012**, *22*, 12651 – 12658.

[19] T. Carell, C. Brandmayr, A. Hienzsch, M. Müller, D. Pearson, V. Reiter, I. Thoma, P. Thumbs, M. Wagner, *Angew. Chem.* **2012**, *124*, 7220 – 7242; *Angew. Chem. Int. Ed.* **2012**, *51*, 7110 – 7131.

[20] J.-M. Lehn, *Angew. Chem.* **2013**, *125*, 2906 – 2921; *Angew. Chem. Int. Ed.* **2013**, *52*, 2836 – 2850.

[21] J. W. Steed, D. R. Turner, K. J. Wallace, *Core Concepts in Supramolecular Chemistry and Nanochemistry*, Wiley, Chichester, **2007**.

Received: June 17, 2014
Published online on September 26, 2014

© 2014 Wiley-VCH Verlag GmbH & Co. KGaA, Weinheim